The Luther Condition for All: Evaluating Colorimetric Camera Design for Personalized Color Imaging

Hao Xie [1,*] and Mark D. Fairchild [1]

[1] Program of Color Science / Munsell Color Science Laboratory, Rochester Institute of Technology
* Corresponding author: hao.xie@mai.rit.edu

Abstract

The Luther condition has been a guideline for colorimetric camera design. However, the standard observer only represents an average observer without considering the inter-observer variability. Thus, there is still potential observer-camera metamerism between a camera colorimetric to the standard observer and an actual observer that has different CMFs. In this work, 1000 sets of CMFs were used to evaluate the RIT camera sensitivity dataset that includes 28 representative cameras. In general, it is found that the camera performances averaged across the individual observers can be predicted from the standard observer. However, the ranking by the standard observer would not be approved by some individuals; therefore a camera less colorimetric to the standard observer can be more colorimetric to an individual observer. And two cameras that are similarly colorimetric to the standard observer can have different levels of variation for the whole population. Furthermore, when the individual observer's CMFs are unknown, the typical color characterization using the standard observer may likely cause higher mismatches between the camera and the individual observer. This work provides theoretical insights for personalized color imaging, where from camera to display, color can be consistently captured and rendered for any individual observer.

Keywords: *Camera Sensitivity, Luther Condition, Color Matching Functions, Individual Difference*

Introduction

Trichromacy, Metamerism, and Color Matching Functions

Human color vision is normally trichromatic; that is, the sensory inputs are based on three types of retinal photoreceptors whose sensitivities respectively peak in the long, medium, and short ranges of visible wavelengths. The physical stimuli are, therefore, transformed from a higher dimensional spectral space to a 3D space, represented as a triplet of cone responses on the retinal level. This dimensional collapse leads to the equivalence condition of different spectra with the same color, which is called metamerism. The standardization of colorimetry is based on metamerism and color matching experiments, resulting in the embodiment of standard observers and their color matching functions (CMFs). Standard observers, such as CIE 1931 2-deg and 1964 10-deg observers, are statistically averaged results from the subjects in color matching experiments. Although they have been serving as decent representative observers and the cornerstone of colorimetry's success in color applications, recent work highlights their deficiency in color-critical situations where narrow-band spectra may be viewed as mismatches for individual observers that have different CMFs due to physiological variations. Knowing an individual's CMFs (together with the availability of spectral information) can help improve personalized color imaging and color management (Asano 2015); the color perceived in the physical world will be captured and rendered faithfully in the digital counterpart for this individual observer. Augmented reality, for example, is among many applications where metamers from different sources may be viewed simultaneously.

Camera Sensitivity and the Luther Condition

Cameras that are expected to record what trichromatic humans see have (at least) three channels with different sensor sensitivities, i.e., RGB cameras. The design of camera sensitivities is a multi-objective optimization process considering quantum efficiency, noise level, colorimetric accuracy, and spatial image quality together, given the practical constraints in manufacturing, etc. (Finlayson & Zhu 2020, Berns 2021). To optimize the colorimetric accuracy alone, the Luther condition has been a guideline for colorimetric camera design, which is fulfilled when a linear transformation between a given set of CMFs and camera sensitivity function exists (Luther 1927). Such a camera can be used as an imaging colorimeter, which can conveniently measure colorimetric information spatially. For any pixel, in other words, the metameric matches for the colorimetric camera are also matches for the corresponding observer. There is no observer-camera metameric failure, and the post-processing applied to the camera raw signals can not distinguish and separate the metamers; thus the tristimulus matches stay undistorted.

To quantify the Luther condition fulfillment and the camera color quality in general, different metrics have been proposed, such as Vora value (Vora & Trussell 1993), metamer mismatch body (Roshan & Funt 2020), and various color difference statistics for a given set of illuminated targets (Berns 2021). They have different theoretical bases and can be interpreted according to the inputs and the calculations. Better metric performances mean the camera is closer to the Luther condition thus more colorimetric. As there are several components in the optical path from the (illuminated) objects to the camera sensor, instead of changing the sensor mosaic, different optimizations are possible to improve the colorimetric camera as a system. Recently, Finlayson and Zhu have computationally demonstrated how to add a physical filter via optimizations in either Vora value or color difference metrics (Finlayson & Zhu 2020). They also considered the physical constraints such as smoothness and transmittance.

Note that the original Luther paper predates the birth of CIE standard observers, which does not preclude itself from being generalized to any individual observer. However, previous work on colorimetric camera design has primarily focused on the standard observer without considering the individual difference in CMFs. While an imaging colorimeter that can report standard CIE XYZ values is desirable, in this paper, we are more interested in personalized color imaging, and the corresponding colorimetric (in a broader sense) camera design. Specifically, the generalized Luther condition, i.e., the colorimetric mapping relation between a given camera-observer pair was evaluated. In addition, the impact of color correction, one critical step in translating camera responses to tristimulus values, was investigated, especially when the individual CMFs were inaccessible. The next section describes the evaluation we conducted, followed by the results and the discussion. The key findings and their implications are summarized in the end.

Evaluation Methods

Dataset and Metrics

To evaluate how colorimetric the commercial cameras can be for each individual observer's CMFs, the RIT camera sensitivity dataset (Jiang et al. 2013), which includes 28 representative cameras and the individual observer dataset from (Asano et al. 2016) were used, from the latter of which 1000 sets of CMFs were generated for 2-deg visual field and age distribution from the US Census 2010. Therefore, 1000-by-28 combinations of colorimetric mapping relations needed to be evaluated. Following the computational procedures and settings (Finlayson & Zhu 2020), the degree of being colorimetric (or

color verisimilitude), was quantified by Vora value and CIELAB-style color differences. For the Vora value, the inputs were one camera's sensitivity versus one individual's CMFs (without dependency on illuminant and reflectance information). When calculating color differences, the SFU datasets of 102 illuminants and 1995 reflectances (Barnard et al. 2002) were used. The camera responses under a given illuminant were transformed to the individual's tristimulus values with a corresponding color correction matrix (CCM) using least-square linear regression, assuming the individual's CMFs and other spectral information were known a priori. Then, the CIELAB-style color differences were calculated across all the illuminants, with the mean results reported. Similarly, the metrics for the 1931 standard observer were repeated for comparison.

Using a Fixed CCM

Since some of the assumptions above could not be practically met, here we consider the case that the individual CMFs were not known; thus, the CCM was not customized during the profiling step. That is, the converted XYZ values from camera responses are instead *standard-observer-referred*. And for calculating the color differences, those standard XYZs were compared against the individual observer's CMFs integrated with the illuminated spectra. Comparing tristimulus values across different CMFs is not common but can be thought of as the physical difference in the color matching weights of XYZ primaries, which is then propagated through the color correction transformation tailored only for the standard observer. The white point in CIELAB was set using the standard CMFs, which only served as a nominal choice. The mean color difference results are reported as done above.

Results and Discussion

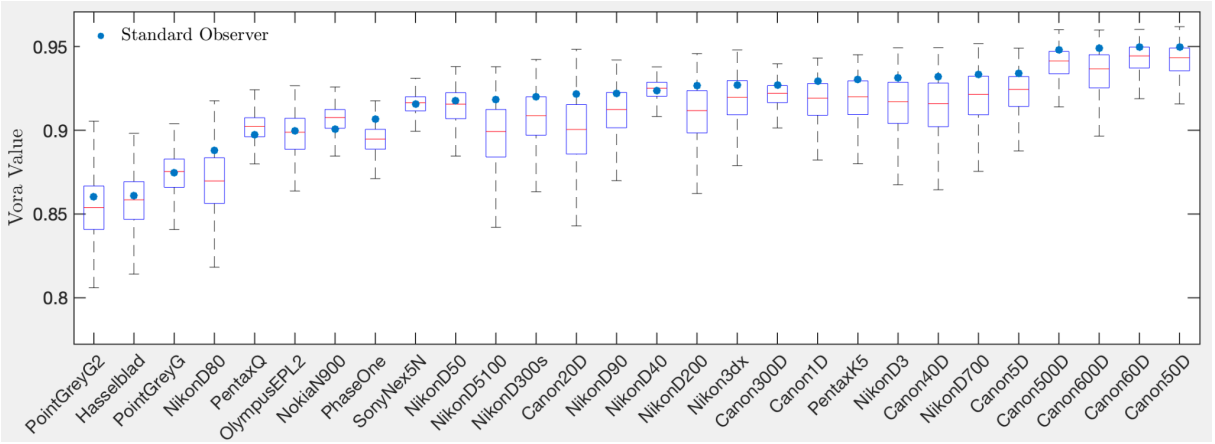

Figure 1. The distributions of Vora values for the 28 cameras are horizontally ordered based on the standard observer's Vora values, shown as blue dots. Each box corresponds to the Vora values of the 1000 observers for each camera. The red line is the median, and the bottom and top edges of the box indicate the 25th and 75th percentiles. If any, roughly a dozen of observer data were removed as outliers for visualization clarity.

As shown in Fig. 1, the Vora values expanded from 0.86-0.95 for the standard observer to 0.78-0.96 for all individual-camera combinations, and similarly, the CIELAB metric increased from 1.10-2.96 to 0.97-4.30 CIELAB units in Fig. 2. In general, the camera performances averaged across the individual observers can be predicted from the standard observer (the blue dots), with the Pearson correlation coefficients of 0.952 and 0.989 for the Vora value and the CIELAB difference, respectively. The standard observer may not fall into the range of 25th and 75th percentiles, especially for the color difference in Fig. 2. This is likely because the CIE 1931 observer is quite different from the average physiologically based observer (Xie et al. 2019). In addition, even if two cameras have similar Vora

values for the standard observer, they may have different magnitudes of variations for a group of individual observers, for example, Nikon D40 versus Nikon D200 in Fig. 1, the former of which should be selected to maximize the larger population's satisfaction.

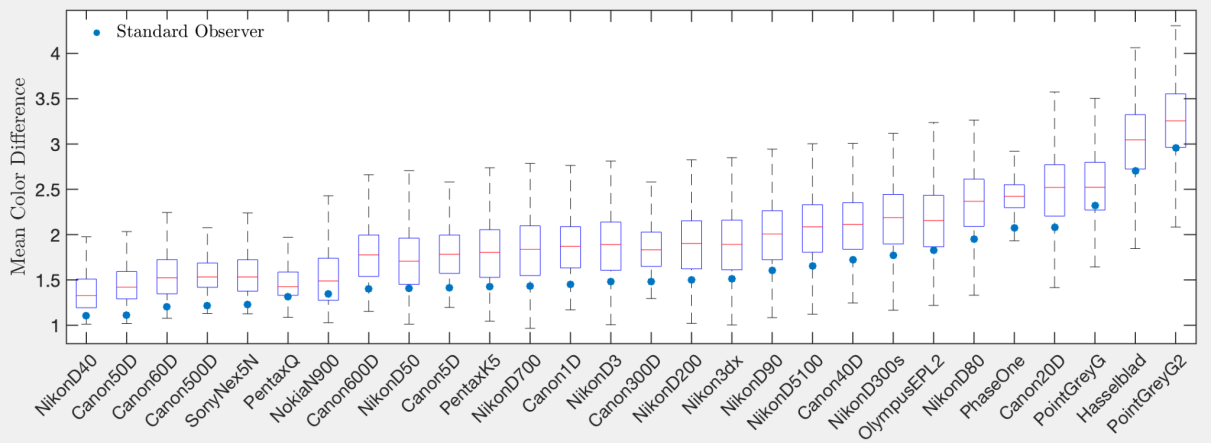

Figure 2. The mean CIELAB color difference distributions are similarly plotted as in Fig. 1.

However, even though the average results confirm the utility of a standard observer, its predictive power might not hold for a given individual observer. Specifically, the lowest Pearson coefficient for the color difference was 0.156, and the worst Kendall's tau correlation for the Vora value was 0.196, meaning that the ranking by the standard observer would not be approved by such individuals, and a camera less colorimetric to the standard observer can be more colorimetric to an individual observer. Figure 3 presents the two extreme observers who can be best and worst predicted by the standard observer, respectively. This observer that has the lowest correlation also overall had lower Vora values, meaning those cameras tested might have higher observer-camera metamerism for them. While Finlayson & Zhu have presented the optimized results for those 28 cameras (Finlayson & Zhu 2020), here we mainly focused on the evaluations, leaving further room for optimization for future work when necessary.

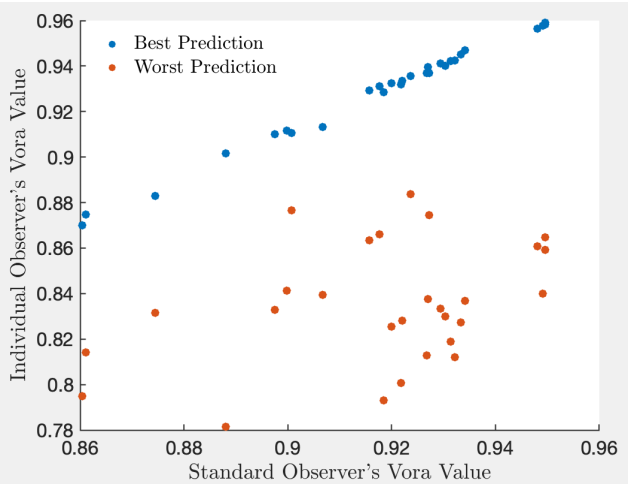

Figure 3. The observers with the highest and lowest Kendall's tau correlation relative to the standard observer in terms of Vora value. The orange points correspond to the observer whose camera ranking had the lowest correlation.

Results of a Fixed CCM

Between the two types of evaluation metrics, which are generally correlated, the Vora value is faster to compute and can generally predict the potential of observer-camera metamerism (Berns 2021); while the higher the better, a value of 0.95 is normally considered very good performance (Finlayson & Zhu 2020). The color difference statistics are probably more interpretable and practical since the calculation procedure can incorporate the steps implemented in the camera pipeline. The practical steps include white balance (estimating the illumination) and color correction. In particular, color correction that is done in camera characterization usually assumes the availability of the spectral information, including the sample targets such as a color-checker, the illumination, and the observer's CMFs. If the CCM is fixed using the standard observer's CMFs, the mean color difference, shown in Fig. 4, for each camera increased by 0.95-1.46 CIELAB units, which were averaged across the 1000 observers. Interestingly, for a given camera, the mean color differences for those 1000 observers did not correlate between a personalized CCM and a standard CCM, suggesting the fixed CCM impacted the results on a group level rather than on an individual level.

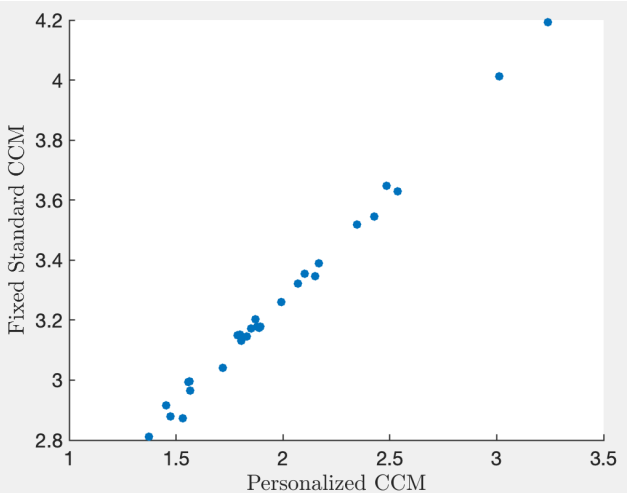

Figure 4. The mean color differences using a fixed CCM against a personalized CCM, each dot as one camera.

Recent work has also presented practical solutions for color correction with more interpolation anchors for different illuminants (Karaimer & Brown 2018) and has shown that the uncertainty of illuminant estimation can significantly impact the colorimetric performance (Tedla et al. 2022). Therefore, our results can be interpreted as upper bounds with ideal illuminant estimation.

Conclusion

In this paper, the general case of the Luther condition is investigated. Instead of considering only the standard observer, the colorimetric relations between any pair of cameras and individual observers were evaluated. Quantitatively, we show that a camera less colorimetric to the standard observer can be more colorimetric to an individual observer. And two cameras that are similarly colorimetric to the standard observer can have different levels of variation for the whole population. Furthermore, when the individual observer's CMFs are unknown, the typical color characterization using the standard observer, although a practically reasonable compromise, may likely cause higher mismatches between the camera and the individual observer.

This work inherits the essentially democratic nature of the Asano model, and with naïve optimism, we hope this approach can help the supply and demand find better matches and probably relax the

single-observer dictated specs. By considering the camera as another metamerism source, this work, in addition to the previous work on observer metamerism, particularly in wide-gamut displays (Xie et al. 2017), provides further theoretical insights for personalized color imaging, where from camera to display color can be consistently captured and rendered for any individual observer.

Acknowledgements

We appreciate the comments from the anonymous reviewers.

References

Asano Y. 2015. Individual Colorimetric Observers for Personalized Color Imaging. *Ph.D. Dissertation*. Rochester Institute of Technology.

Asano, Y., Fairchild, M. D., & Blondé, L. 2016. Individual colorimetric observer model. *PLoS ONE* 11(2): e0145671.

Barnard, K., Martin, L., Funt, B., & Coath, A. 2002. A data set for color research. *Color Research & Application* 27(3): 147-151.

Berns, R. S. 2021. Predicting Camera Color Quality. In: *Archiving Conference*, 61-64.

Finlayson, G. D., & Zhu, Y. 2020. Designing color filters that make cameras more colorimetric. *IEEE Transactions on Image Processing* 30: 853-867. [Code available on Github: https://github.com/zhedazhu1012/Filterdesign]

Jiang, J., Liu, D., Gu, J., & Süsstrunk, S. 2013. What is the space of spectral sensitivity functions for digital color cameras?. In: *IEEE Workshop on Applications of Computer Vision (WACV)*, 168-179.

Karaimer, H. C., & Brown, M. S. 2018. Improving color reproduction accuracy on cameras. In: *Proceedings of the IEEE Conference on Computer Vision and Pattern Recognition*, 6440-6449.

Luther R. 1927. Aus dem Gebiet der Farbreizmetrik. *Z. Tech. Phys.* 8: 540-558.

Roshan, E., & Funt, B. 2020. Color Sensor Accuracy Index Utilizing Metamer Mismatch Radii. *Sensors* 20(15): 4275.

Tedla, S., Wang, Y., Patel, M., & Brown, M. S. 2022. Analyzing color imaging failure on consumer-grade cameras. *JOSA A* 39(6): B21-B27.

Vora, P. L., & Trussell, H. J. 1993. Measure of goodness of a set of color scanning filters. *J. Opt. Soc. Am. A* 10(7): 1499-1508.

Xie, H., Rodríguez-Pardo, C. E., & Sharma, G. 2017. Multiobjective optimization for color display primary designs. *Journal of Electronic Imaging* 26(6): 063013.

Xie, H., Farnand, S. P., Murdoch, M. J., Park, J. S., & Min, B. 2019. Color Mismatches across Commercial Displays: Modeling the Effect of Observer Metamerism. In: *SID Symposium Digest of Technical Papers*, 1374-1377.